

Analysis of Dynamics and Vibration Characteristics of a Binary Wing Model

Jiaqi Liu, Liangqiang Zhou*

School of Mathematics, Nanjing University of Aeronautics and Astronautics, Nanjing, China

Email: 2173883650@qq.com, *zqlqrex@sina.com

How to cite this paper: Liu, J.Q. and Zhou, L.Q. (2026) Analysis of Dynamics and Vibration Characteristics of a Binary Wing Model. *Journal of Applied Mathematics and Physics*, **14**, 1789-1801.
<https://doi.org/10.4236/jamp.2026.145087>

Received: April 10, 2026

Accepted: May 12, 2026

Published: May 15, 2026

Copyright © 2026 by author(s) and Scientific Research Publishing Inc. This work is licensed under the Creative Commons Attribution International License (CC BY 4.0).

<http://creativecommons.org/licenses/by/4.0/>



Open Access

Abstract

This paper investigates the dynamics and flutter characteristics of a two-degree-of-freedom airfoil with cubic (third-order) structural stiffness nonlinearity, which captures the hardening behavior essential for predicting limit cycle oscillations and Hopf bifurcation in aeroelastic systems. Herein, the “binary wing” (or “binary airfoil”) specifically refers to the classic two-degree-of-freedom typical-section airfoil model, which idealizes the wing as a rigid profile undergoing plunge (heave) and pitch motions, capturing the fundamental aeroelastic coupling. The equations of motion are derived using Lagrange’s principle, and a state-space representation is formulated by incorporating an aerodynamic model. The variation of system eigenvalues with flow velocity is analyzed to determine the linear flutter critical speed. Numerical simulations are employed to verify the existence of subcritical flutter. The research demonstrates that the binary airfoil with nonlinear stiffness can exhibit stable limit cycle oscillations at subcritical speeds, with distinct patterns in modal coupling and flutter frequency evolution with velocity.

Keywords

Aeroelasticity, Flutter, Binary Airfoil, Nonlinear Stiffness, Subcritical Hopf Bifurcation, Limit Cycle Oscillation

1. Introduction

This Aerodynamic elastic fluttering of aircraft wings represents a classic and critical dynamic challenge in aerospace engineering. This phenomenon arises from complex energy interactions among structural inertial forces, elastic forces, and aerodynamic forces. When critical conditions are reached, the system loses stability and develops self-excited vibrations known as fluttering. If left uncontrolled, such instability can rapidly lead to structural fatigue or even catastrophic failure.

Consequently, predicting and extending flutter boundaries (critical velocities) remains a core safety indicator in aircraft design [1] [2].

Traditional linear flutter theories (such as Theodorsen $p - kU_g U < U_g$ theory and French theory) are based on assumptions of linear structural stiffness and small disturbances, enabling effective prediction of “linear critical flutter velocity.” However, real-world aircraft wing systems often exhibit unavoidable nonlinear factors, including free-play clearance, geometric nonlinearity caused by large deformations (cubic stiffness), material nonlinearity, and aerodynamic nonlinearity under high attack angles (e.g. dynamic stall) [3] [4]. These nonlinear factors significantly alter the system’s dynamic behavior, resulting in substantial deviations between actual stall speeds and linear predictions. Particularly concerning is subcritical flutter phenomenon—where nonlinear Hopf bifurcation causes stable limit cycle oscillations (LCO) at incoming flow velocities. This poses severe flight safety risks, as aircraft may abruptly enter violent vibration modes within speed profiles deemed “safe” by designers [5] [6].

While quadratic nonlinearities (e.g., $k\alpha^2$) are often associated with static aeroelastic instabilities such as wing divergence or post-buckling, cubic nonlinearities ($k\alpha^3$) are required to model dynamic instabilities like limit cycle oscillations (LCO) and Hopf bifurcation. Therefore, to investigate the dynamic instability of primary concern (*i.e.*, flutter and LCO), this study focuses on the cubic nonlinear stiffness model. In this study, we adopt a cubic stiffness model to accurately capture the nonlinear flutter behavior observed in typical-section airfoils under high-speed flight conditions.

Historically, Theodorsen [7] established the classical linear unsteady aerodynamic theory in the 1930s, laying the foundation for flutter analysis. However, with the development of high-speed aircraft, nonlinear effects became increasingly prominent. Dowell *et al.* [8] [9] systematically conducted theoretical research on nonlinear aerodynamic elasticity during the 1970s-1980s, introducing modern nonlinear analysis methods such as bifurcation theory and chaos dynamics into this field. Lee and Price [10] conducted detailed numerical and experimental studies on binary wings with structural nonlinearity, uncovering abundant bifurcation and chaotic phenomena. Entering the 21st century, research on nonlinear aerodynamic elasticity placed greater emphasis on engineering applications. Guo and Chen [11] systematically analyzed the conditions for supercritical and subcritical Hopf bifurcation in wings with cubic nonlinearities, as well as their impact on LCO amplitude.

The binary wing (typical airfoil) model serves as the fundamental physical framework for aerodynamic elasticity research. Its ability to elucidate modal coupling mechanisms between heave and pitch degrees of freedom has made it widely adopted in theoretical and experimental studies of nonlinear flutter phenomena. International research trends indicate that nonlinear aerodynamic elasticity response analysis has expanded beyond single nonlinear factors (e.g., clearance and cubic stiffness) to encompass cutting-edge domains such as multiphysics cou-

pling, quantified parameter uncertainty, active control systems, and smart material applications [12] [13]. Particularly in subcritical flutter research, accurately predicting onset boundaries, evaluating impacts on flight safety, and developing effective suppression strategies have become key research priorities and challenges.

In the evolution of analytical methods, early-stage research primarily relied on time-domain numerical integration techniques (e.g., Runge-Kutta method) for phenomenon observation. With advancements in computational mechanics, frequency-domain approaches (such as harmonic balance method [HB]), descriptor function methods, and central manifold reduction theory were introduced, enabling analytical understanding of nonlinear dynamics mechanisms [14]. The application of normal form theory further provided robust mathematical tools for determining and simplifying nonlinear bifurcation types [15]. In recent years, data-driven methods (including eigenorthogonal decomposition [POD] and deep learning) have been applied to order reduction modeling and response prediction for complex nonlinear systems [16].

In China, significant progress has also been made in nonlinear flutter research. Yang Qiwei and Zhou Jifu [17] conducted in-depth studies on bifurcation and chaotic behaviors of nonlinear flutter in binary wings, revealing the influence of nonlinear stiffness parameters on system dynamic characteristics. Ding Qian *et al.* [18] applied Wash-out filter technology to control wings with cubic nonlinear stiffness, successfully transforming subcritical flutter into supercritical flutter. Niu Yaobin *et al.* [19] investigated nonlinear energy well suppression methods for nonlinear wing flutter in high-speed aircraft gaps. These studies not only advanced the development of nonlinear aeroelasticity theory but also provided crucial technical support for aerospace engineering practices in China.

From an engineering application perspective, in-depth research on subcritical flutter holds significant practical implications. Modern aircraft design extensively employs innovative concepts such as composite materials, high aspect ratio wings, and deformable wings, which exhibit more pronounced nonlinear mechanical behaviors [20]. Concurrently, the continuous expansion of flight envelopes (e.g., hypersonic operations and high maneuverability) amplifies the impact of nonlinear aerodynamic elasticity. Therefore, establishing accurate nonlinear dynamic models, developing efficient analytical methods, and achieving precise prediction and effective control of subcritical flutter are critical for ensuring flight safety and enhancing aircraft performance.

This study focuses on a binary wing model with nonlinearity in pitch direction stiffness. The innovative contributions are primarily reflected in three aspects: First, at the methodological level, we established an integrated linear/nonlinear stability analysis framework combining eigenvalue analysis, Routh-Hurwitz criterion, and numerical bifurcation (Hopf bifurcation) detection, thereby enhancing systematic analysis capabilities. Second, in terms of phenomenon validation, rigorous numerical simulations clearly demonstrated the existence of subcritical Hopf bifurcation phenomena, confirming the system's dynamic characteristics of

generating stable limit cycle oscillations (LCO) below linear critical velocity. Finally, regarding mechanism exploration, quantitative analysis revealed how nonlinear stiffness coefficients influence flutter boundaries, bifurcation types, and LCO amplitude-frequency characteristics. The study uncovered the “jumping” behavior of modal coupling and flutter frequencies with incoming flow velocity variations, providing new insights into the role of stiffness nonlinearity in aeroelastic instability mechanisms.

The innovation of this paper lies in: systematically studying the flutter characteristics of rigid nonlinear binary wings from three perspectives—theory, numerical simulation, and methodology—with a particular focus on subcritical flutter, a highly hazardous phenomenon in engineering practice. By integrating cutting-edge nonlinear dynamics theory with the practical needs of China’s aeronautical engineering, it provides new perspectives and technical references for research in related fields.

2. Kinetic Modeling

2.1. Simplified Model of Binary Wings

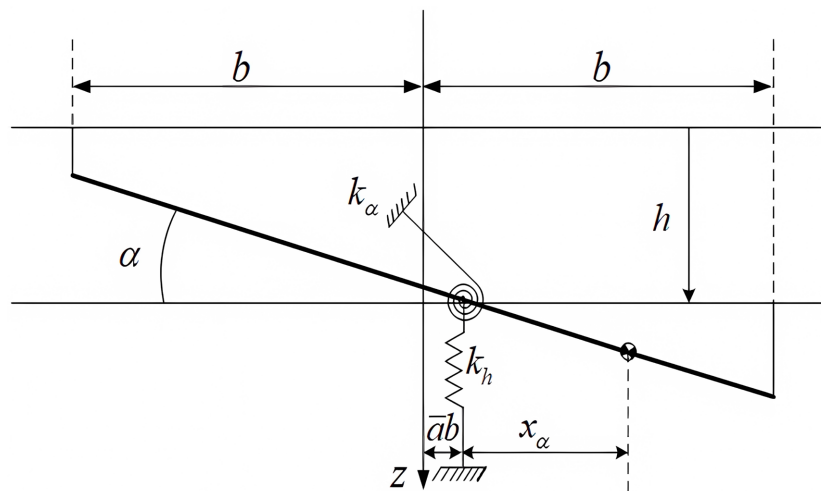


Figure 1. Model.

As shown in **Figure 1**, the binary wing is simplified into a rigid body model: with a half chord length of b , the distance from the center of mass to the midpoint of the wing chord is $a \cdot b$ (where a represents the percentage of the center of mass relative to the midpoint of the wing chord), and the distance between the center of mass and the center of mass is $x_\alpha \cdot b$. h and α denote the vertical displacement of the wing (along the chord direction) and the pitch angle (rotation angle around the center of mass), respectively. \dot{h} , \ddot{h} , $\dot{\alpha}$, and $\ddot{\alpha}$ correspond to velocity and acceleration, respectively.

2.2. Derivation of Motion Equations

According to Lagrange’s principle, the motion equation of a binary wing with

stiffness nonlinearity can be expressed as:

$$\begin{cases} m_T \ddot{h} + m_W x_\alpha b \ddot{\alpha} + c_h \dot{h} + k_h h = -L(\alpha, h, \dot{\alpha}, \dot{h}) \\ m_W x_\alpha b \ddot{h} + I_\alpha \ddot{\alpha} + c_\alpha \dot{\alpha} + k_\alpha(\alpha) \alpha = M(\alpha, h, \dot{\alpha}, \dot{h}) \end{cases} \quad (1)$$

In the formula:

- m_T represents the total system mass, m_W wing mass, and I_α pitch rotation inertia;

- c_h, c_α The damping coefficients for heave and pitch, and k_h, k_α the stiffness coefficients for heave and pitch;

- L, M For aerodynamic forces (lift) and moments, and $k_\alpha(\alpha) = k_{\alpha 0} + k_{\alpha 1} \alpha + k_{\alpha 3} \alpha^3$ for nonlinear pitch stiffness (the cubic term reflects the nonlinear variation of stiffness with pitch angle)

2.3. Aerodynamic Model

The aerodynamic forces are modeled using a quasi-steady approximation. This simplification is commonly adopted in the study of nonlinear aeroelastic stability and bifurcation phenomena, as it retains the essential coupling between structural motion and aerodynamic forces while significantly reducing computational complexity. The model is intended to be valid for incompressible flow and moderate reduced frequencies, where the effects of wake vorticity and aerodynamic lag are secondary to the nonlinear structural response of primary interest in this study.

The aerodynamic L, M forces (lift force and torque) are modeled under quasi-steady assumptions, expressed as:

$$\begin{cases} L = \rho U^2 b C_{L\alpha} \alpha_{eff} \\ M = \rho U^2 b^2 C_{M\alpha} \alpha_{eff} \end{cases} \quad (2)$$

The effective angle of attack α_{eff} incorporates the coupling between heave velocity and pitch angular velocity:

$$\alpha_{eff} = \alpha + \frac{\dot{h}}{U} + \left(\frac{1}{2} - a\right) b \frac{\dot{\alpha}}{U} \quad (3)$$

In the formula,

ρ denotes the air density, U denotes the incoming flow velocity, and $C_{L\alpha}, C_{M\alpha}$ denotes the aerodynamic coefficient of lift and torque relative to the pitch angle.

2.4. State Space Model

By combining the motion Equation (1) with the aerodynamic models

$X = [h, \alpha, \dot{h}, \dot{\alpha}]^T$ (2) and (3), and introducing state vectors, the system is transformed into a state equation:

$$\dot{X} = A(U)X + Q(X, X) + C(X, X, X)$$

Among:

- $A(U)$ is the linear system matrix (related to velocity U) that describes the linear characteristics of the system.

-The nonlinear term $Q(X, X)$ represents the quadratic stiffness contribution (set to zero in this study), while $C(X, X, X)$ captures the cubic stiffness nonlinearity, which is the primary driver of the Hopf bifurcation and limit cycle behavior observed in the system.

Simplified state equation:

$$\dot{X} = A(U)X + C(X, X, X)$$

3. Linear Flutter Analysis (Eigenvalue Method)

3.1. Eigenvalues and Stability Criteria

The eigenvalues $A(U)\lambda = \sigma + j\omega$ of a linear system matrix determine the stability of the system:

-The system is asymptotically $\sigma < 0$ stable if all the real parts of the eigenvalues are negative.

-If the real part of the eigenvalue $\sigma > 0$ exists, the system becomes unstable (flutter occurs);

-If the real part of a conjugate $\sigma = 0$ U_g eigenvalue corresponds to a linear critical flutter velocity, it indicates the critical flutter condition.

3.2. Variation Pattern of Eigenvalues with Velocity

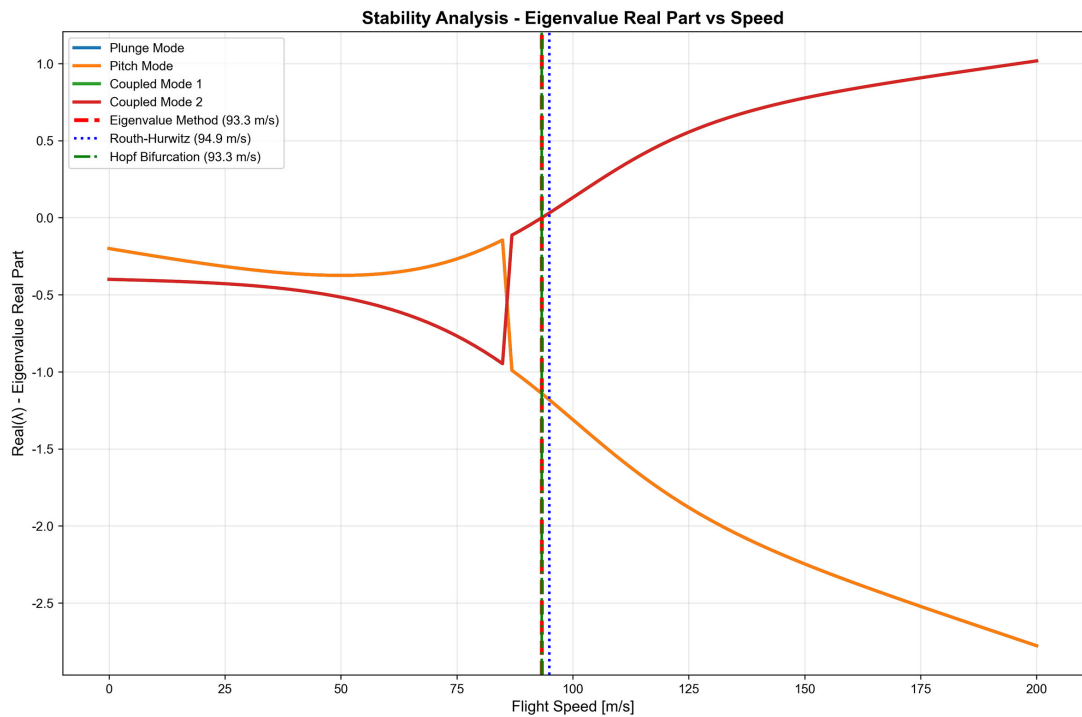


Figure 2. (Plot of the real part of eigenvalues versus velocity).

The variation of the real part of modal eigenvalues U with incoming flow velocity is demonstrated across different modalities:

-Rise-fall mode (blue curve): The real part remains consistently negative, indi-

cating stable system motion during ascent and descent phases.

-Pitching mode (orange curve): The real part is negative U at low speeds, and as the speed approaches the linear critical velocity, the real part gradually increases and crosses the imaginary axis (transitioning from negative to positive).

The eigenvalue crossing at 93.3 m/s corresponds to a Hopf bifurcation induced by cubic structural nonlinearity.

Coupled modes (green and red curves): At low speeds, the real U part is negative. As the speed increases, the real parts of a pair of conjugate eigenvalues gradually increase, eventually crossing the imaginary axis and triggering flutter.

Combining the Routh-Hurwitz criterion (blue dashed line in **Figure 2**) with Hopf bifurcation analysis (green dashed line $U_g \approx 93.3\text{ m/s}$ $\sigma = 0$ in **Figure 2**), the linear critical flutter velocity is approximately (consistent with the velocity obtained by the eigenvalue method).

3.3. Root Locus Analysis

Root Locus Plot (Eigenvalue Trajectory vs Speed)

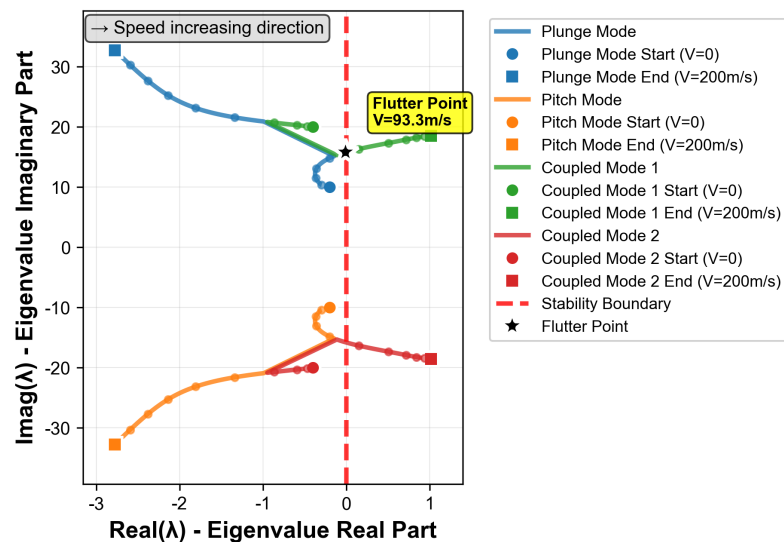


Figure 3. (Root locus diagram).

As shown in **Figure 3**, the trajectory of eigenvalues varying with velocity is illustrated:

-At low speeds ($U = 0$), all eigenvalues are located in the left half-plane of the complex plane (stable region);

-Flutter Point: Hopf bifurcation point (cubic nonlinearity).

As the $U \approx 93.3\text{ m/s}$ parameter increases, the trajectories of a pair of conjugate eigenvalues (corresponding to coupled modes) approach the imaginary axis and cross it at a certain time (the red dashed line represents the stability boundary), triggering flutter.

The trajectories of other modalities (heave, pitch) remained consistently within the left hemispheric plane or maintained stability after flutter onset.

4. Nonlinear Vibration Analysis (Subcritical Vibration Verification)

4.1. Numerical Simulation of Subcritical Vibration

To validate subcritical flutter (steady limit cycle motion occurring when the system operates below the linear critical velocity), the fourth order Runge-Kutta method was employed to solve the state Equation (4), with initial conditions set as specified and the incoming flow velocity maintained below the linear critical velocity.

The system exhibits stable limit cycle motion at subcritical speeds: the amplitudes of displacement (h, α) and velocity $(\dot{h}, \dot{\alpha})$ tend to stabilize over time, with a constant phase difference, indicating the presence of self-excited oscillations (fluttering).

To further confirm that the observed LCOs originate from a subcritical Hopf bifurcation rather than merely a nonlinear LCO below the linear flutter speed, the sensitivity to initial conditions is examined. Numerical integration from a very small initial disturbance (e.g., $X_0 = [0.01, 0.1, 0, 0]^T$) at the same subcritical velocity ($U = 0.8U_g$) shows that the response decays to the trivial equilibrium. In contrast, the finite-amplitude initial condition reported above triggers a sustained LCO. This bistability—a locally stable equilibrium coexisting with a stable limit cycle for the same flow parameters—is the hallmark of a subcritical Hopf bifurcation, indicating the presence of an unstable limit cycle branch separating the basins of attraction. This confirms the hazardous nature of the flutter, as finite disturbances can trigger large-amplitude oscillations even below the linear stability boundary.

4.2. Vibration Frequency and Modal Coupling Characteristics

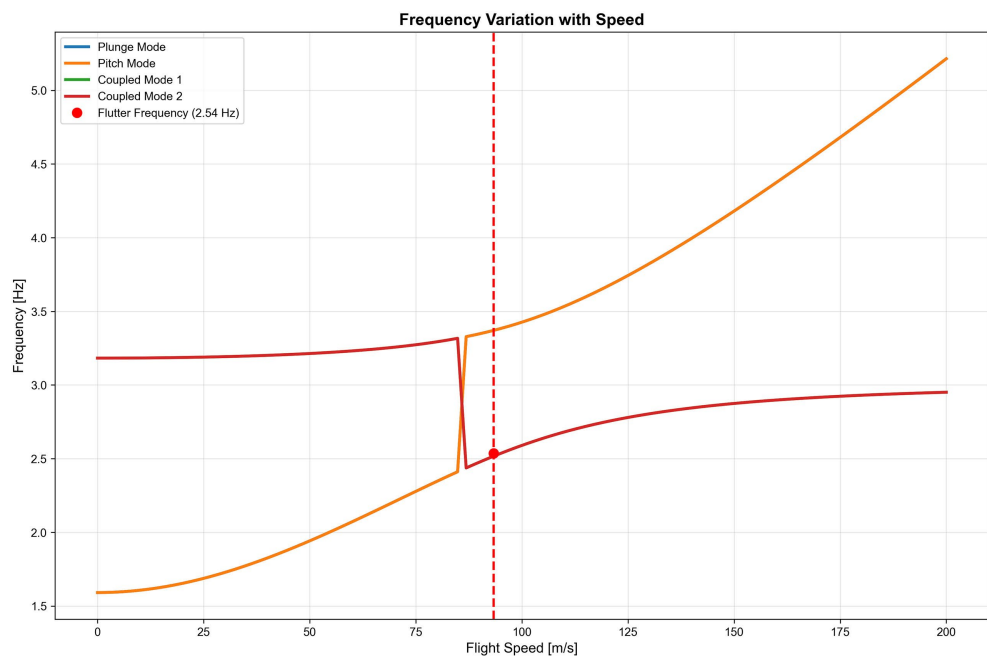


Figure 4. Vibration frequency versus velocity plot.

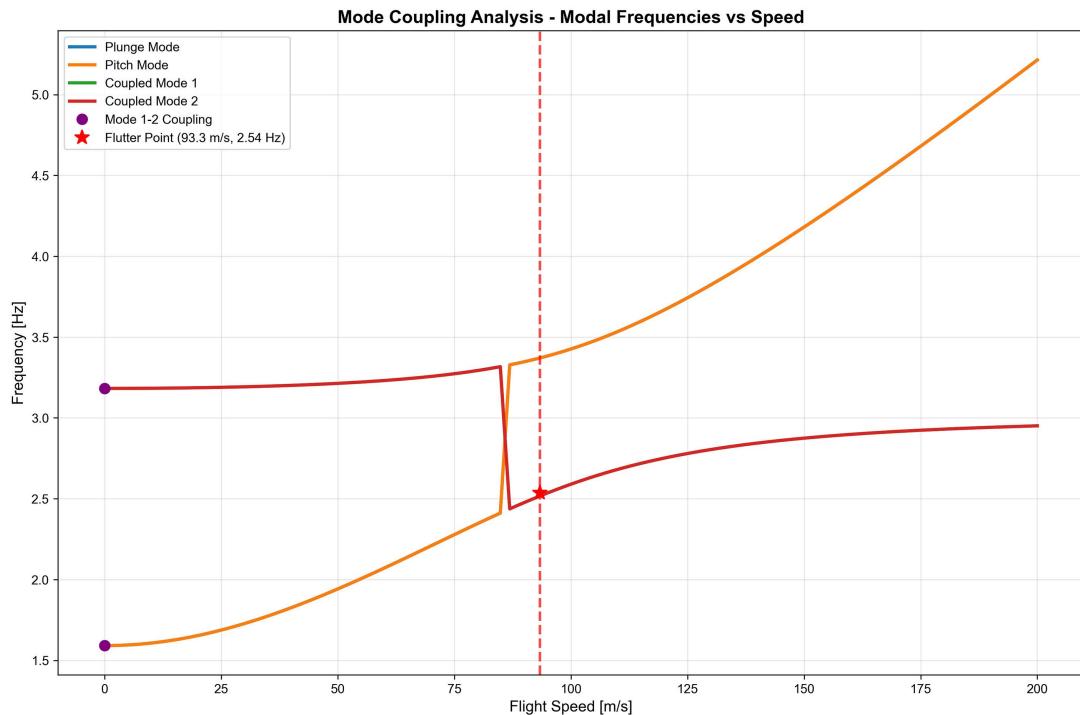


Figure 5. Modal coupling analysis diagram.

Figure 4 and **Figure 5** reveal the relationship between frequency and velocity:

- Modal frequency of oscillation (blue curve): increases slowly with increasing velocity and remains largely unaffected by nonlinear effects;

- Pitch modal frequency (orange curve): shows a significant increase with increasing speed, reflecting the coupling effect of aerodynamic damping and stiffness;

- Coupled modal frequencies (green and red curves): The frequencies of low-frequency coupled modes (green) and high-frequency coupled des (red) exhibit a “jumping” characteristic with velocity variation, showing a frequency coupling point (purple dot) near the flutter velocity, corresponding to a flutter frequency of approximately (red dot in **Figure 4**).

5. Conclusions

This study investigates the dynamics and flutter characteristics of a binary wing model with nonlinear stiffness by establishing nonlinear dynamic equations and state space models. Through integrated application of eigenvalue analysis, Routh-Hurwitz criterion, numerical bifurcation analysis, and numerical integration methods, we systematically examine the system’s behavior. The research identifies a linear flutter critical velocity of approximately 93.3 m/s. Significantly, numerical simulations confirm the existence of subcritical flutter phenomena: when operating below this critical velocity (e.g., 0.8 Ug), nonlinear stiffness induces subcritical Hopf bifurcation, resulting in stable limit cycle oscillations. This study confirms that cubic structural nonlinearity is essential for capturing the dynamic flutter in-

stability in binary wings, as evidenced by the presence of a Hopf bifurcation and limit cycle oscillations. Quadratic nonlinearities, while relevant for static instability, are insufficient to explain the observed oscillatory behavior.

Further analysis reveals modal coupling mechanisms during flutter onset and demonstrates the “jumping” characteristic of flutter frequency (approximately 2.54 Hz) varying with incoming flow velocity. This study provides theoretical foundations and numerical methodologies for instability analysis and safety design of aeroelastic systems with nonlinear structures, enhances understanding of subcritical flutter hazards, and offers critical engineering insights for aircraft aeroelastic safety.

Acknowledgements

The project was supported from the “University-Level Innovation Training Program” at Nanjing University of Aeronautics and Astronautics (NO. 20251028700967X).

Conflicts of Interest

The authors declare no conflicts of interest regarding the publication of this paper.

References

- [1] Bisplinghoff, R.L., Ashley, H. and Halfman, R.L. (1955) *Aeroelasticity*. Addison-Wesley.
- [2] Fung, Y.C. (2002) *An Introduction to the Theory of Aeroelasticity*. Dover Publications.
- [3] Dowell, E.H., Crawley, E.F., Curtiss Jr., H.C., *et al.* (2015) *A Modern Course in Aeroelasticity*. 5th Edition, Springer.
- [4] Lee, B.H.K., Price, S.J. and Wong, Y.S. (1999) Nonlinear Aeroelastic Analysis of Airfoils: Bifurcation and Chaos. *Progress in Aerospace Sciences*, **35**, 205-334. [https://doi.org/10.1016/s0376-0421\(98\)00015-3](https://doi.org/10.1016/s0376-0421(98)00015-3)
- [5] Guo, H.L. and Chen, Y.S. (2012) Supercritical and Subcritical Hopf Bifurcation and Limit Cycle Oscillations of an Airfoil with Cubic Nonlinearity in Supersonic/Hypersonic Flow. *Nonlinear Dynamics*, **67**, 2637-2649. <https://doi.org/10.1007/s11071-011-0177-1>
- [6] Hao, S.H. and Chen, Y.S. (2007) Study on Non-Zero Equilibrium Point Limit Cycle Flutter of Cubic Nonlinear Wings. *Science and Technology in Engineering*, **7**, 4327-4330.
- [7] Theodorsen, T. (1935) General Theory of Aerodynamic Instability and the Mechanism of Flutter. NACA Report No. 496. https://digital.library.unt.edu/ark:/67531/metadc53413/m2/1/high_res_d/19800006788.pdf
- [8] Dowell, E.H., Edwards, J. and Strganac, T. (2003) Nonlinear Aeroelasticity. *Journal of Aircraft*, **40**, 857-874. <https://doi.org/10.2514/1.134>
- [9] Dowell, E.H. and Ilgamov, M. (1988) *Studies in Nonlinear Aeroelasticity*. Springer.
- [10] Lee, B.H.K., Jiang, L.Y. and Wong, Y.S. (1999) Flutter of an Airfoil with a Cubic Restoring Force. *Journal of Fluids and Structures*, **13**, 75-101. <https://doi.org/10.1006/jfls.1998.0190>

-
- [11] Guo, H.L. and Chen, Y.S. (2012) Supercritical and Subcritical Hopf Bifurcation and Limit Cycle Oscillations of an Airfoil with Cubic Nonlinearity in Supersonic/Hypersonic Flow. *Nonlinear Dynamics*, **67**, 2637–2649.
- [12] Marzocca, P., Librescu, L. and Silva, W.A. (2002) Aeroelastic Response of Nonlinear Wing Sections Using a Functional Series Technique. *AIAA Journal*, **40**, 813-824. <https://doi.org/10.2514/2.1735>
- [13] Zhao, Y.H. and Hu, H.Y. (2007) Pneumatic Elasticity Mechanics and Control. Science Press.
- [14] Liu, L. and Dowell, E.H. (2005) Harmonic Balance Approach for an Airfoil with a Freeplay Control Surface. *AIAA Journal*, **43**, 802-815. <https://doi.org/10.2514/1.10973>
- [15] Irani, S., Khayyeri, K. and Dardel, M. (2011) Bifurcation in a 3-DOF Airfoil with Cubic Structural Nonlinearity. *Journal of Sound and Vibration*, **330**, 1211-1226.
- [16] Brunton, S.L., Proctor, J.L. and Kutz, J.N. (2016) Discovering Governing Equations from Data by Sparse Identification of Nonlinear Dynamical Systems. *Proceedings of the National Academy of Sciences*, **113**, 3932-3937. <https://doi.org/10.1073/pnas.1517384113>
- [17] He, D.P. and Huang, W.T (2019) Limit Cycle Flutter and Chaotic Motion of a Binary Airfoil System. *Journal of Guangxi Normal University (Natural Science Edition)*, **37**, 87-95. (In Chinese) <https://doi.org/10.16088/j.issn.1001-6600.2019.03.010>
- [18] Ding, Q. and Wang, D.L. (2004) Structural and Aerodynamic Nonlinear Wing Vibration Analysis. *Journal of Dynamics and Control*, **2**, 1-6. (In Chinese) <https://doi.org/10.3969/j.issn.1672-6553.2004.03.005>
- [19] Niu, Y.B., Wang, Z.W. and Huang, W. (2024) Suppression of Nonlinear Energy Traps for Nonlinear Wing Flutter in High-Speed Aircraft Clearance. *Journal of National University of Defense Technology*, **46**, 79-85. (In Chinese)
- [20] Dimitriadis, G. (2017) Introduction to Nonlinear Aeroelasticity. Wiley. <https://doi.org/10.1002/9781118756478>

Parameter Appendix Table

Appendix A. Description of Physical Significance

This table lists the core parameters used in the two-degree-of-freedom aeroelastic analysis of a wing section. Parameters are divided into “Input Parameters” and “Derived Parameters.” Input parameters are based on classical aeroelastic theory and standard characteristics of 2D airfoils; derived parameters are calculated using fundamental mechanical equations for subsequent equation of motion formulation and numerical simulation. All parameters are referenced to the half-chord length $b = 1.0$ m.

Appendix B. Parameter Table

Category	Parameter Name	Symbol	Value	Unit	Description / Source
Input Parameters	Half-chord length (reference length)	b	1.0	m	Baseline geometric length for non-dimensionalization.
	CG-to-EA relative position	x_α	0.2	—	Dimensionless parameter describing longitudinal position of CG relative to elastic axis (positive for rearward).
	Mass ratio	μ	100	—	Ratio of wing mass to aerodynamic mass, controls inertial effects.
	Radius of gyration ratio	r_α	0.5	—	Dimensionless parameter determining pitch moment of inertia.
	Heave natural frequency	ω_h	10	rad/s	Natural frequency of the heave (plunge) mode.
	Pitch natural frequency	ω_α	20	rad/s	Natural frequency of the pitch mode.
	Air density	ρ	1.225	kg/m ³	Standard sea-level atmospheric density.
Derived Parameters	Lift curve slope	$c_{l\alpha}$	6.283185307179586	rad ⁻¹	Close to theoretical value 2π , represents 2D airfoil lift characteristics.
	Wing mass	m	384.8451000647497	kg	Calculated by $m = \mu * (\rho * b^2)/2$.
	Pitch moment of inertia	I_α	96.21127501618743	kg·m ²	Calculated by $I_\alpha = m * (r_\alpha * b)^2$.
	Heave linear stiffness	k_h	38484.51000647497	N/m	Calculated by $k_h = m * \omega_h^2$.
Analysis Results	Pitch linear stiffness	$k_{\alpha 0}$	38484.51000647497	N·m/rad	Calculated by $k_{\alpha 0} = I_\alpha * \omega_\alpha^2$.
	Flutter speed	U_g	93.31739122136042	m/s	Critical flutter speed obtained from linear flutter analysis.
	Flutter frequency	ω_g	2.5352717259898636	Hz	Vibration frequency at flutter onset.
	Critical flutter mode	—	3	—	Mode index of the dominant flutter mode from eigenvalue analysis.
	Hopf bifurcation point	—	Detected	—	Critical condition for system stability transition.

Appendix C. Rationale for Key Parameter Selection

Geometric & Structural Parameters: $b, x_\alpha, \mu, r_\alpha, \omega_h, \omega_\alpha$ are selected based on

standard textbook examples (e.g., Aircraft *Aeroelasticity*) to ensure benchmark comparability.

Aerodynamic Parameters: ρ follows international standard values; $c_{l\alpha} = 2\pi$ corresponds to an ideal inviscid, incompressible 2D airfoil, facilitating theoretical validation.

Frequency Ratio: $\omega_h/\omega_a = 0.5$ is chosen to induce frequency locking, making the flutter analysis representative of coupled-mode instability.